

OncoPeptTUME™ – A novel *in-silico* approach to model the tumor microenvironment and predict treatment efficacy and long-term survival benefits for immunotherapy applications

Background

Cancer immunotherapy is now established as a major therapeutic modality, and 70% of all cancer patients are estimated to receive some form of immunotherapy treatment as a part of their disease control by 2025. Cancer immunotherapy drugs elicit their anti-tumor immune response in a subset of the treated patients by activating CD8 T-cells and provide sustainable and long-lasting benefit in a few. Recently significant efforts have been devoted to understanding the factors that influence response to immuno-therapy or contribute to the development of resistance to therapy. While it is appreciated that many different tumor cell- intrinsic and extrinsic features, including the tumor microenvironment, driver gene mutations, host genetics, microbiome and environmental factors modulate response to immune checkpoint inhibitors¹, the tumor microenvironment ecosystem could be a major contributor in regulating response to immunotherapy and development of resistance^{2,3}. Ongoing efforts to characterize the tumor microenvironment to stratify patients for immunotherapy, and find biomarkers of response often use methods that are limited by 1) availability of adequate tumor tissue from needle biopsy material; 2) restricted set of cell surface and phenotypic markers to analyze the cellular composition with limited tissue availability, and 3) loss of tissue integrity during processing for downstream analysis. Recently, single-cell transcriptomics has enabled studies to analyze the heterogeneity in a population of cells from a tissue and define gene expression signatures in the tumor microenvironment^{4,5}, but the quality of data generated is still governed by the sample collection method and quality of RNA (determined by the presence of viable cells). Alternatively, genomic methods that use deconvolution to assess relative enrichment of different cells types can be utilized to understand the composition of the tumor microenvironment, but that approach can also be limited in utility by biases introduced by dependencies in the cell type⁶. Taken together, a robust method of studying the tumor microenvironment to identify the molecular signature is still needed. To this end, Signios Bio has developed OncoPeptTUME™, a genomic solution that utilizes its highly cell-type specific proprietary minimal gene expression signature for 8 different immune cells. The expression of genes for a given signature was transformed to produce a cell-type specific immune score that was used to quantitate the relative proportion of cell types present in the complex tumor microenvironment. In this white-paper we highlight a) how the proprietary gene expression signatures were generated and validated, b) robustness of our gene signatures compared to other existing methods in identifying cell types of interest c) utility of the OncoPeptTUME™ in defining immunogenicity (via immune score assignments) of tumors and predicting prognosis and long-term survival benefits based on the immune signatures of the tumors.

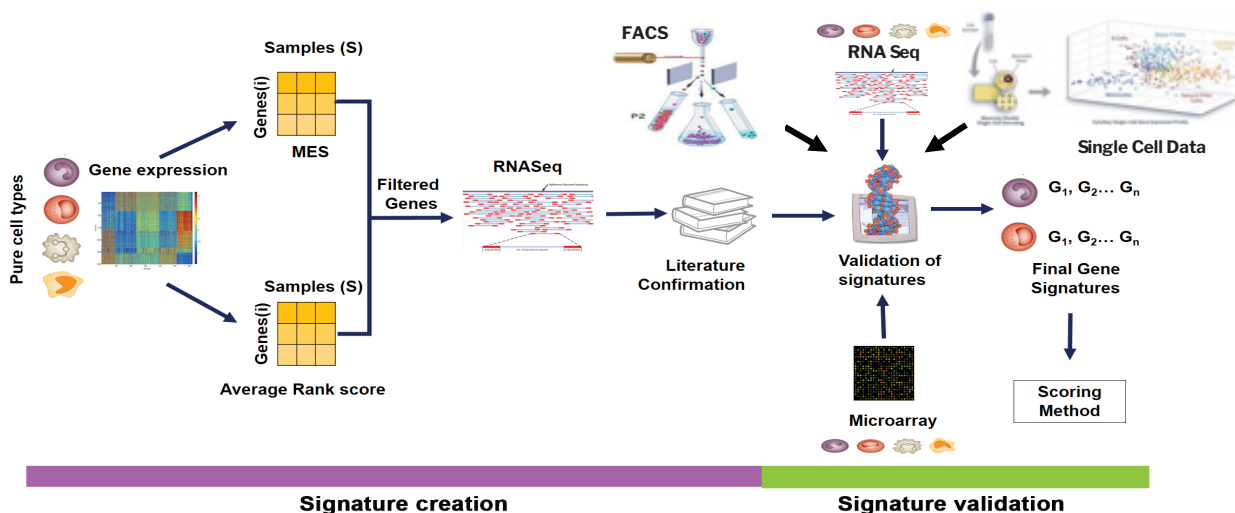


Figure 1. Workflow for building the minimal gene expression signatures (MGESPs) : The microarray gene expression data contd.

was used to calculate the ARS and MES scores (measures of specificity and plasticity of a gene in each of the pure cell types respectively). The signatures were further refined by curation and validated on an independent set of microarray and RNA-Seq data from pure cell populations.

Creating immune specific gene expression signatures

To generate unique gene expression signatures for specific immune cell-type, a large number of microarray and RNA-seq datasets of pure immune cells from 4 different platforms were analyzed (Table 1). Genes showing significantly lower expression plasticity- high MES (Marker Evaluation Score) and higher expression specificity for a given cell-type high ARS (Average Rank Score) were included in the signature and were refined further by literature review and data curation (Figure 1). We applied single-cell Gene Set Enrichment Analysis ssGSEA to determine cell-type specific scores associated with each gene signature. Briefly, normalized gene expression values were rank-normalized and rank-ordered, and the score for a given signature was calculated based on the position of the genes in the rank-ordered list. We employed a multi-pronged approach to create highly specific signatures corresponding to different cell types present in the tumor microenvironment as shown in Figure 1.

Table 1 - Datasets used to generate the gene expression signatures

Immune Response		Innate						Adaptive					Total
Cell type		NK	Neutrophils	Monocytes	Macrophage	M2	M1	Treg	DC	CD8	CD4	B cell	
Building the signature		149	457	462		385		72	411	189	619	1545	4289
Validation	RNA seq	14	20	20	-	-	-	5	-	20	20	20	103
	Microarray	81	114	186	45	45	32	130	153	92	73	158	1445

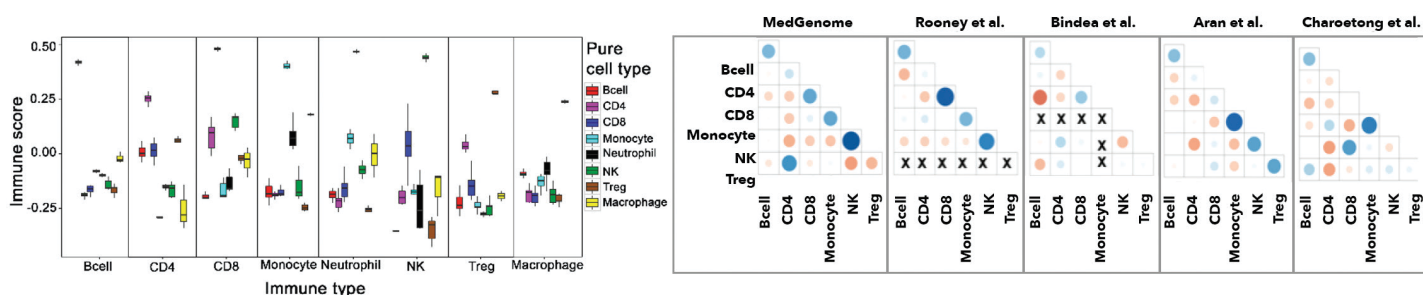


Figure 1. Validation of gene expression signatures : (A) Validation of MGESPs on RNA-Seq data represented as boxplots with cells on the x-axis and immune scores on the y-axis. Each facet represents the immune score (y-axis) calculated for a specific cell-type plotted on the x-axis. A higher score was observed for cognate cell type compared to non-cognate cells. (B) Performance comparison of MGESPs with other published signatures on FACS data^{8,9,10}. Figure shows correlation between MGESP scores with FACS- based enumeration of cells. Size of the bubble indicates sample number, and blue circle represents positive correlation and red circle represents negative correlation.

Validation of the gene expression signatures

The specificity of gene signatures was validated on highly purified cell-type data (cells with >90% purity) obtained from various published studies (Table 1). The raw data were downloaded from public databases and processed using in-house microarray and RNA-seq analysis pipelines. In contrast to non-cognate cells, our signatures yielded a relatively higher score for the cognate cell type. We also tested whether the different number of reads from different experiments will affect the immune score for a specific cell type, and we observed that the scores were stable across the whole range of data size, indicating that our scoring method is robust for analyzing and comparing tumors whose transcriptomes were sequenced at different depth in different experiments.

Creating immune specific gene expression signatures

To test the utility of the OncoPeptTUME™ in defining immune signatures and assigning immune scores to cancers for interest, we decided to utilize RNA-seq data from 33 cancers from the TCGA datasets and performed a tumor microenvironment analysis using the OncoPeptTUME™ pipeline. Based on our analyses, each of the tumors have an immune score assigned to them, and categorized into quartiles, to represent high (Q1) versus low (Q4) level of immune infiltration. (Figure 3a) . We also identify the relative enrichment of the 8 different immune cell types in the cancers (Figure 3b). Our analyses revealed interesting findings about the immune compositions of the different tumor types. For example, we find that Kidney renal cell carcinoma (KIRC) being an immune-sensitive tumor had a high infiltration of all the immune cell types except Treg cells, whereas kidney renal papillary cell carcinoma (KIRP) showed lesser infiltration of most immune cell types. Interestingly, kidney chromophobe cancer (KICH) showed a high infiltration of NK cells and low infiltration of other cell types, previously reported by immunohistochemistry analysis. In conclusion, the analyses using OncoPeptTUME™ shed interesting insights into the immune landscape of different cancers ¹⁰.

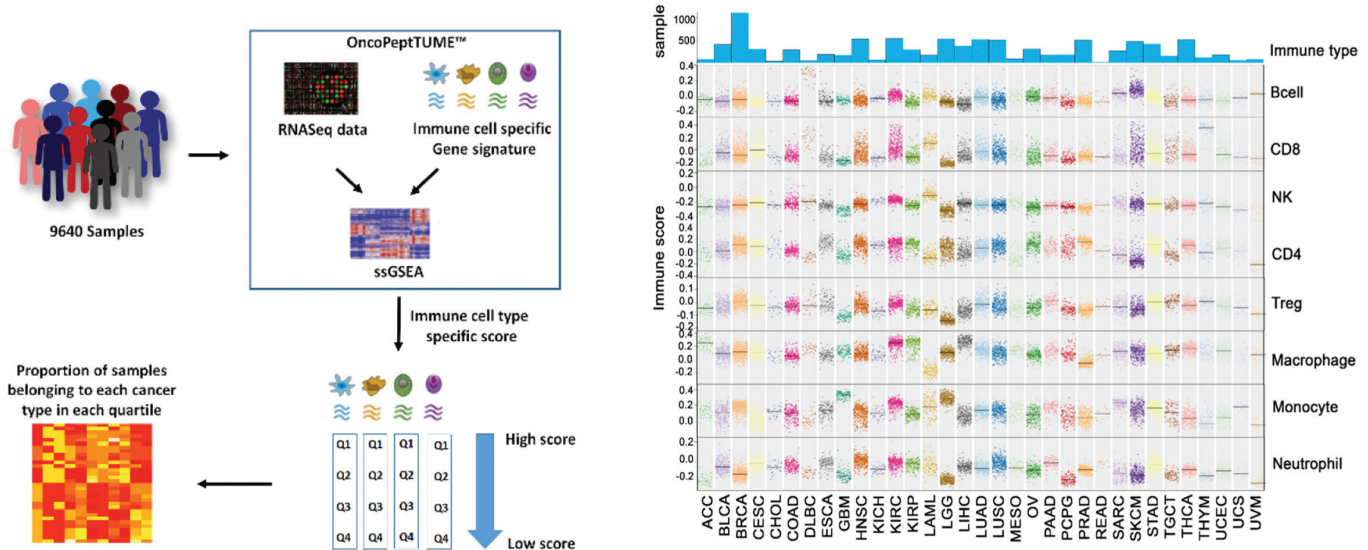


Figure 3. Comprehensive analysis of the immune landscape of 9640 tumors across 33 cancers using OncoPeptTUME™ : (A) Shows the OncoPeptTUME™ workflow to process 9640 TCGA datasets to identify cancers of the highest immune filtration for a particular immune cells type. MGESP-derived score for each cell type was calculated for each of the tumors and arranged into quartiles. Q1 implies highest level of infiltration of a certain immune cell type into the tumor and Q4 implies lowest level of expression. (B) Representation of the relative enrichment of 8 different immune cell types in all the different cancer type.

OncoPeptTUME™ identifies effect of immune cell infiltration on long-term survival in TCGA cancer-types

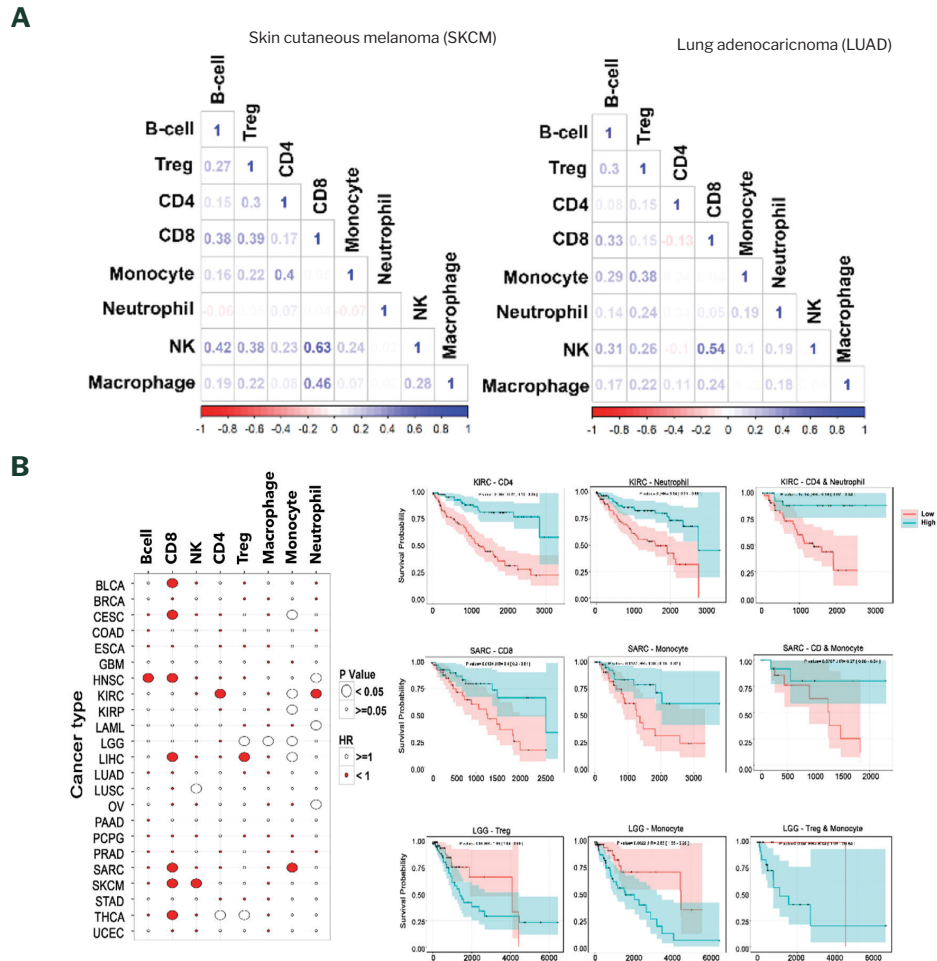


Figure 4. (A) Representation of the correlation of immune infiltration seen in SKCM and LUAD cancers. (B) Correlation between infiltration of different immune cells and patient survival. For each cancer survival benefit between the top and 20% tumor samples infiltrated by specific immune cells was compared. Size of the bubble shows sample number, red and blue indicates good and poor prognosis respectively, and significant associations (p -value < 0.005) are shown. (C) Effect of combined infiltration of two cell-types on patient survival represented as Kaplan Meier Plots for selected cancers.

Utility of OncoPeptTUME™ analysis in predicting response to immune checkpoint inhibitors treatment

We then decided to apply the immune scoring to understand the immunogenicity of the tumor samples, and assess efficacy to immunotherapy treatment. In the current field of immunotherapy, presence of high levels of tumor infiltrating leukocytes in solid tumors is often correlated with better survival¹². It has also been suggested that different cancers benefit from infiltration of different types of immune cells. For example, the co-occurrence of T cells and NK cells in tumors enhances the efficacy of cancer immunotherapy drugs¹³. However, there has been no systematic analysis of co-infiltration of multiple immune cells across different cancers. Therefore, we used the TCGA data to investigate the landscape of co-infiltrating immune cells in all 33 cancers. For cancers that have shown a good response to immune checkpoint inhibitors (SKCM, KIRC, bladder carcinoma (BLCA, LUAD, head and neck squamous cell carcinoma (HNSCC)), a positive correlation between CD8+ T-cells and NK cells, was observed with the strongest correlation detected in SKCM and LUAD (Figure 3C). In addition, using the MGESPs, we were able to uncover that survival benefit was positively or negatively affected by the co-infiltration of multiple immune cells. As an example, kidney renal carcinoma (KIRC) benefited from the infiltration of CD4+ T-cells and neutrophils, whereas sarcomas (SARC) showed a survival benefit from co-infiltration of CD8+ T-cells and monocytes. Conversely, LGG showed poor survival from the co-infiltration of Treg cells and monocytes. We also observed that the combined benefit of co-infiltration by CD8+ T-cells + neutrophils in KIRC, or CD4+ T-cells monocytes in SARC exceeded the survival benefit observed from the infiltration of an individual type of cell.

OncoPeptTUME™ analysis reveals functional features of CD8 + T cells associated with long term survival in many cancers

To further investigate, how different immune cells co-operate with each other or act against each other to impact survival, we clustered 9120 TCGA tumors (patients with survival data available) into clusters based on the combined infiltration of eight different immune cell types (Figure 5A). The tumor samples clustered into four major groups according to the relative content of eight different immune cells (Fig. 5A). Cluster 3 and 4 had high CD8+ T-cell infiltration compared to cluster 1 & 2 (Figure 5B). Next, we analyzed cluster-4 with high CD8+ T-cells to investigate the mechanism of survival. Of the 1554 cases in cluster 4, 1200 belong to live and the remainder are deceased. We utilized this data set to probe the functional state of the CD8+ T-cells in both the groups, and found that while both groups have expression of activation marker PD-1, only the deceased group was enriched for markers of exhausted and anergic CD8+ T-cells expressing *CTLA4*, *LAG3* and *TIM3* (Figure 5C). Further, CD8+ T-cells in the alive group showed higher expression of genes belonging to TCR signaling pathway supporting their activated phenotype (Figure 5D). Interestingly, the markers of long-term survival identified by OncoPeptTUME™ are the same that determines response to checkpoint blockade¹⁴, strongly demonstrating the utility of OncoPeptTUME™ in cancer immunotherapy clinical trials.

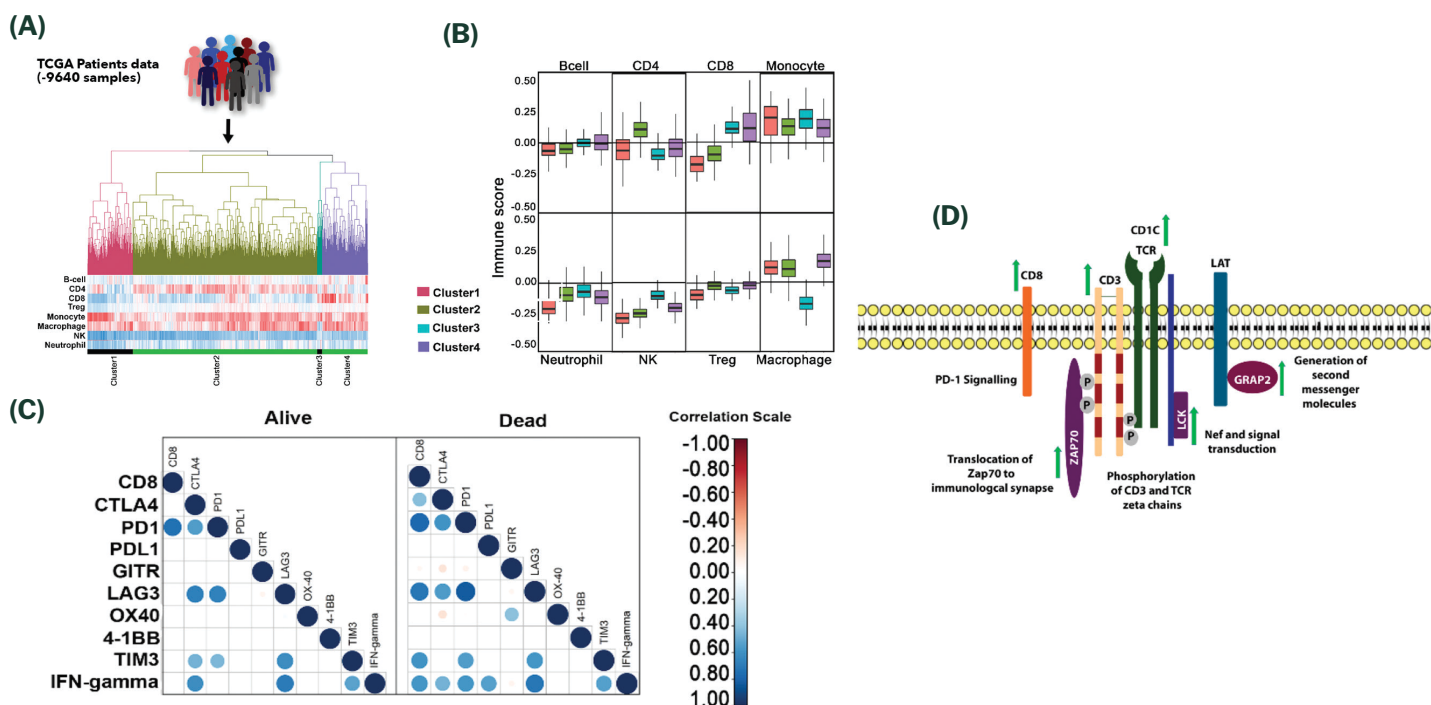


Figure 5. (A) Clustering of TCGA patient samples using hierarchical clustering using immune scores derived using the minimal gene expression. Four major clusters are represented in different colors with their corresponding immune cell type infiltration represented as a heatmap below the dendrogram. (B) Boxplot showing the variation in the distribution of immune infiltration scores for each immune cell type across the four clusters. (C) Correlation of expression between the infiltration of CD8+ T-cells vs the anergic and exhaustion markers with the CD8+ T-cell in the two groups. (D) Cartoon representation of the genes upregulated in the TCR signaling pathway in the alive subjects of cluster-4.

References

1. Chen, D.S. and I. Mellman. (2017). Elements of cancer immunity and the cancer-immune set point. *Nature*, 541(7637): p. 321-330.
2. Hanahan, D., and Coussens, L. M. (2012). Accessories to the crime: functions of cells recruited to the tumor microenvironment. *Cancer Cell*, 21(3), 309–322.
3. Quail, D., and Joyce, J. (2013). Microenvironmental regulation of tumor progression and metastasis. *Nature medicine*, 19(11), 1423–1437.
4. Tirosch, I., Izar, B., Prakadan, S. M., Wadsworth, M. H., Treacy, D., Trombetta, J. J., Rotem, A., et al. (2016). Dissecting the multicellular ecosystem of metastatic melanoma by single cell RNAseq. *Science (New York, N.Y.)*, 352(6282), 189–196.
5. Zheng, C., Zheng, L., Yoo, J.-K., Guo, H., Zhang, Y., Guo, X., Kang, B., et al. (2017). Landscape of Infiltrating T Cells in Liver Cancer Revealed by Single-Cell Sequencing. *Cell*, 169(7), 1342–1356.e16.
6. Avila Cobos, F., Vandesompele, J., Mestdagh, P., and De Preter, K. (2018). Computational deconvolution of transcriptomics data from mixed cell populations. *Bioinformatics (Oxford,England)*.
7. Newman, A.M., Liu, C.L., Green, M.R., Gentles, A.J., Feng, W, Xu, Y., Hoang, C.D., et al. (2015). Robust enumeration of cell subsets from tissue expression profiles. *Nature*, 12, 453-457.
8. Aran, D., Hu, Z., and Butte, A. J. (2017). xCell: digitally portraying the tissue cellular heterogeneity landscape. *Genome Biology*, 18, 220.
9. Bindea, G., Mlecnik, B., Tosolini, M., Kirilovsky, A., Waldner, M., Obenauf, A. C., Angell, H., et al. (2013). Spatiotemporal dynamics of intratumoral immune cells reveal the immune landscape in human cancer. *Immunity*, 39(4), 782–795.
10. Charoentong, P., Finotello, F., Angelova, M., Mayer, C., Efremova, M., Rieder, D., Hackl, H., et al. (2017). Pan-cancer Immunogenomic Analyses Reveal Genotype-Immunophenotype Relationships and Predictors of Response to Checkpoint Blockade. *Cell Reports*, 18(1), 248–262.
11. Geissler, K., Fornara, P., Lautenschläger, C., Holzhausen, H.-J., Seliger, B., and Riemann, D. (2015). Immune signature of tumor infiltrating immune cells in renal cancer. *Oncoimmunology*, 4(1), e985082.
12. Badalamenti, G., Fanale, D., Incorvaia, L., Barraco, N., Listì, A., Maragliano, R., Vincenzi, B., et al. (2019). Role of tumor-infiltrating lymphocytes in patients with solid tumors: Can a drop dig a stone? *Cellular Immunology*, 343, 103753.
13. Melero, I., Rouzaut, A., Motz, G. T., and Coukos, G. (2014). T-Cell and NK-Cell Infiltration into Solid Tumors: A Key Limiting Factor for Efficacious Cancer Immunotherapy. *Cancer Discovery*, 4(5), 522–526.
14. Riaz, N., Havel, J. J., Makarov, V., Desrichard, A., Urba, W. J., Sims, J. S., Hodi, F. S., et al. (2017). Tumor and Microenvironment Evolution during Immunotherapy with Nivolumab. *Cell*, 171(4),934–949.e15.

 info@signiosbio.com

 (888) 440-0954

 348 Hatch Drive, Foster City, CA 94404, USA